

Investigation of the Feasibility of Increasing the Tail-grouting Zone during Mechanized Tunneling in Sandy Soils

Faezeh Barri¹, Hamid Chakeri^{1*}, Hamed Haghkish², Milad Manafi³

¹ Department of Mining Engineering, Sahand University of Technology, 5331817634, Tabriz, Iran

² Department of Construction Management, Islamic Azad University, 5157944533, Tabriz, Iran

³ Department of Mining Engineering, Amirkabir University, 1591634311, Tehran, Iran

* Corresponding author, e-mail: chakeri@sut.ac.ir

Received: 28 August 2023, Accepted: 18 October 2023, Published online: 08 November 2023

Abstract

Nowadays, excavation in urban environments can have many risks; one of these hazards is improper tail-grouting of Earth Pressure Balance Machine (EPBM) and the consequent ground surface settlement. Failure to fill the tail space with suitable grout significantly affects the surface displacements. Injecting more grout to penetrate deeper around the tunnel will play a more effective role in reducing displacements and permeability of the soil. Therefore, experimentally investigation of the feasibility of increasing the tail-grouting zone during excavation around the tunnel space and the effect of this penetration on the amount of ground surface displacements is the main purpose of this paper. Thus, experimental tests were performed with different grout injection pressure and the effect of each of the pressure on the penetration depth of grout into the soil new laboratory model were examined. Then to study the effect of the grout penetration depth on surface settlement to determination of the adequate amount of grout injection pressure a numerical modeling of Tabriz metro line 2 by FLAC3D software were completed. For this purpose, the results of the laboratory tests (the penetration depth of grout) were used in numerical modeling. The results indicated that the amount of penetration in the implemented granulation has increased due to the increase in pressure, so doubling the pressure causes a 30% increase in grout penetration in the surrounding soil. The results of numerical studies showed that increasing the range of injection in the modeling causes a significant reduction (80 percent) in the ground surface settlement.

Keywords

tail-grouting, numerical modeling, laboratory modeling, injection pressure, ground surface settlement

1 Introduction

Nowadays, the need for new excavations has increased with the expansion of urbanization and the increase in utilizing urban rail transportation, especially the subway. Meanwhile, tunneling with a Tunnel Boring Machine (TBM) has become popular due to its advantages, such as high mechanization, safety, and environmental compatibility [1].

On the other hand, excavation of tunnels and underground spaces in urban areas is highly sensitive. Considering the crossing of such tunnels through the city roads with heavy traffic, it is necessary to prevent any settlement and destruction of the ground surface, which, apart from safety problems, leads to disruption of traffic on the ground surface and damage or destruction of nearby buildings [2].

An annular void remains between the retaining system and the soil during the tunneling with a TBM, whether in soft or hard soil. This void can cause significant ground

settlement and must be filled quickly using a proper grouting method [3]. The system in the tail of TBM to fill this void is illustrated schematically in Fig. 1 [4].

Generally, grout is used to fill these types of voids in the ground to increase resistance against deformation, increase adhesion, increase shear strength and uniaxial compressive strength, or finally to reduce permeability and water entering the tunnel, protecting the tunnel lining

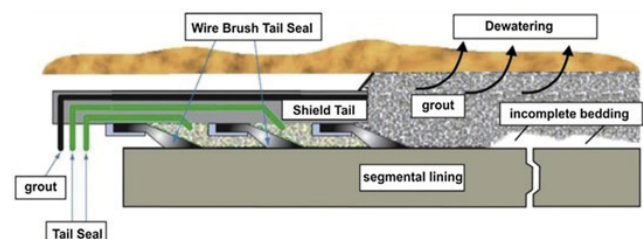


Fig. 1 Shield tail [4]

against aggressive factors in water and soil, high stability in the case of high-water velocity [5–7].

Most utilized grouts are cement-based because they are easily accessible and inexpensive. Two-component grouts are increasingly used worldwide due to their many advantages and good compatibility with different types of soils. Quick hardening in these grouts reduces the settlement risk [3, 8]. Two-component grout comprises components A and B, pumped separately through separate pipes and mixed at the injection point. Component A is a cement mortar designed to be chemically and physically stable. This component usually comprises cement, water, bentonite, and retarder/plasticizer. Component B is an accelerator mixture added to Component A just a few centimeters before the grout injection nozzle. Component B is usually made up of Sodium silicate solution [8]. The two-component grout has an initial setting time and high initial strength and is generally used in water-rich layers [9]. Examples of projects using two-component grout for injecting behind the segment could be mentioned as Line C in Rome (Italy), Arroyo Maldonado hydraulic tunnel in Buenos Aires (Argentina), LAT tunnels in Singapore, Sparvo Tunnel (Italy), Belchen Tunnel in Switzerland, Nanjing Yangtze River Crossing Tunnel (China). Various researchers have conducted many laboratory and numerical studies regarding the impact of different parameters on the characteristics of the grout behind the segment, among which we can mention the following researchers: Mansour [10], Abu-Krishna [11], Greenwood [12], Kasper and Meschke [13], Nagel and Meschke [14], Lambrughi et al. [15], Li et al. [16], Oh and Ziegler [17], Shah et al. [18], Ochmański et al. [19], Loganathan and Poulos [20], Komiya et al. [21], Liu et al. [22].

Vonk [6] researched to investigate the impact of injecting grout behind the segment to balance the soil stress and minimize deformations around the tunnel.

Mohammadzamani et al. [23] investigated the effect of the hydro-mechanical properties of the injection material on both the short-term and long-term behavior of the tunnel. Various properties of the injection material are examined in this study using a three-dimensional Finite Element method, including the thickness of the injection layer, permeability, stiffness, hardening ratio (E_1 (the initial stiffness)/ E_{28} (the final stiffness of the grouting material)), shrinkage, and creep behavior. The results indicated that the weaker strength properties of the newly injected grout could lead to more deformation. A similar process can be observed for the excess pore pressure around the excavated

tunnel. The hardening ratio of the grout was the most influential factor in reducing the surface deformations up to 75% when increased from 0.3 to 0.5. These researchers stated that more rigid grout transfers all the load from adjacent soil into the segmental linings, and more apparent deformations in different parts are unavoidable due to the lack of flexibility and stress reduction in this state.

Xue et al. [24] simulated the mechanical behavior of ground around the TBM after injection using a 3D Ubiquitous-Multiple-Joint (UMJ) model. The effects of different injection parameters were analyzed in this study, including the w/c ratio, injection pressure, distance of boreholes, and borehole orientation. They indicated that the w/c ratio has the most critical impact on the quality of injection. Increasing the injection pressure from 2 to 4 MPa has caused a slight increase in the volume of grouted rock mass. However, the volume increase is significant near the excavation front.

Liu et al. [25] investigated the effect of self-compacting grout in filling and injection on the adjacent stone structures in excavating with a double shield TBM through numerical and experimental simulations. They suggested that injecting this kind of grout could provide a perfect role for the self-bearing capacity of the surrounding rock. In this paper, the support time, and mechanical properties of self-compacting concrete backfilling material (SCCBM) were analyzed based on the simulations of a TBM manufacturing process. Generally, filling the SCCBM with optimal retention time can reduce the deformation of the surrounding rock of the TBM and increase the rock's stability. The timelier the filling of SCCBM is, the lower the deformation and risk of failure in the surrounding land.

Sharghi et al. [3] examined the mechanical properties of grout, such as compressive strength, modulus of elasticity, and Poisson's ratio. In this study, experiments were conducted with different ratios of material, and finally, the effect of each component on the properties was investigated. Also, numerical modeling of Line 2 of the Tabriz metro has been developed by FLAC3D software to examine the effect of grout characteristics on the surface settlement. Finally, according to the numerical results, they concluded that an excessive increase of cement in grout would only result in additional costs without significantly impacting the settlement control. Hence, preparing a grout with the same strength as the surrounding soil to fill the tail space is adequate and will control the surface settlement. A few parameters were examined in the numerical model of this study, including the surface pressure,

injection pressure, and grout characteristics, and the estimated results were compared with each other and with the instrumentation test results and field tests.

Chakeri et al. [26] studied the impact of thickness of the tail space on the maximum surface settlement and the surface settlement curve. They mainly focused on the effects of the above parameters on surface settlements. The effects of three parameters, including the injection pressure, grout characteristics, and gap thickness, were investigated by FLAC3D. The modeling results were compared with those obtained from experimental and field measurements. The results of numerical modeling showed that: the FD model predicted the maximum surface settlement equal to 8.81 mm and 88.1 mm for the case of EPBM in the grout with high and low properties, respectively. The surface settlement decreased with the increase in injection pressure.

Rahmati [27] conducted laboratory experiments to examine the characteristics of two-component grout, such as flowability, bleeding, gelling time, and uniaxial compressive strength. The results indicated that increasing bentonite and cement leads to an increase in the marsh funnel time and, thus, a decrease in the flowability of grout. Increasing the bentonite and decreasing the w/c ratio decreased the bleeding of fresh grout. Increasing the amount of cement and sodium silicate (accelerator) and reducing the w/c ratio increased the amount of UCS. Bentonite also increased the short-term compressive strength but decreased it in the long term. Gelling time has a direct relationship with the amount of sodium silicate and an inverse relationship with its ratio (silicon dioxide/silicon oxide). Increasing the dose of sodium silicate increased the gelling time. Decreasing the sodium silicate ratio increased the gelling time. The modulus of elasticity decreased with the increase of the w/c ratio. The final strength of grout increases with the increase of lateral pressure. The compressive strength of grout increases in the finite state (Triaxial test) with the increase of bentonite (only short-term), sodium silicate, and silicon dioxide to sodium oxide ratio. Like the finite state. Data obtained from triaxial tests is used to determine characteristics such as shear strength and apparent adhesion of different materials. Applying the obtained parameters in the numerical models could simulate the grout behavior in a more realistic state.

In the study conducted by Oreste and Spagnoli [28], the effective impact of the mechanical properties of the filling materials on the stability of the tunnel support systems is analyzed. These researchers showed that the hardness of the filler material behind the segment (elastic modulus) affects

the maximum applied stress on the segment. This effect increases with the elastic modulus of the soil around the tunnel. However, the filling materials will not impact the segmental support if the elastic modulus is less than 500 MPa.

Todaro et al. [29] showed in their study, which focused on the effect of bentonite on the grout, that the swelling index and the Atterberg liquid limit are valuable parameters in predicting the results of grout bleeding and its compressive strength. A simple test in this study found that bentonite is of critical importance in the two-component grout and affects the behavior of both components, Component A and the hardened grout, even though the bentonites are not identical. The role of bentonite in stabilizing Component A and its effect in reducing bleeding was confirmed.

In a study using real construction data, Todaro et al. [30] analyzed the intrinsic properties of two-component grout. The results indicated that although different mix designs are now used in construction projects, determining the appropriate test model can be important in describing the two-component grout.

Todaro and Pace [31] have investigated six two-component grout mix designs with different elastic properties using geophysical measurements. Their research showed that the grouts with bentonite have a higher dynamic modulus than those without bentonite. In addition, the final analysis of the experimental data provided an analytical relationship to calculate the shear wave velocity for each of the six grouts at different ages.

The present study investigates the effect of injection pressure and grout penetration by building a new laboratory model to examine the impact of increasing the grout injection zone behind the segment. Then the results were compared with the real data obtained from Line 2 of the Tabriz metro. In the next step, the effect of injection depth on the ground surface settlement has been investigated using numerical modeling. So, the main purpose of this article is to determine the amount of grout penetration around the tail space behind the segment and examine its effect on the ground surface settlement considering the amount of penetration and mixing percentage.

2 Laboratory investigation of the penetration rate of grout in soil

As mentioned earlier, the amount of grout penetration into the surrounding soil based on the injection pressure is one of the main parameters in the grout performance behind the segment. Obviously, better sealing, increasing soil resistance, and reducing the settlement could be assured

by greater penetration of grout into the soil around the tunnel. Therefore, the effect of pressure on grout penetration into the soil has been investigated in this study by building a particular device for that purpose.

A laboratory injection system was designed and built to examine the grout penetration. The structure and dimensions of the injection simulation system are illustrated in Fig. 2. The test system consists of an injection simulation test frame, an injection system, and a monitoring system. In the injection process, the grout is injected into the center of the circular space inside the plexiglass frame with height 40 cm and diameter of 12.2 cm and spreads from the central position parallel to the plexiglass sheet. Two polyethylene covers are present at both ends of the grout chamber. The top cover includes an opening for pouring grout into the chamber and another opening for applying pressure through the compressor. A stress loading system by two air compressors loaded the pressure of injected medium before starting the injection operation to guarantee the completely dense state of the injected medium.

To perform the test, the two components of grout, A (grout) and B (Accelerator), are poured into their specific tanks. Then each component is sent to a tee shown in Fig. 2 with a pipe and injected into the soil tank after mixing. The entry amount for each component is adjusted based on the mix design by release valves installed under the tanks. The land pressure is provided by an air compressor attached to the soil tank. The air compressor attached to the grout and quick-setting tanks is utilized to give the injection pressure for the grout. The grout mix enters the circular space inside

the soil tank through the injection hole and subsequently spreads into the soil layer. The pressure sensors inside the soil and grout tanks, indicated in Fig. 2, are utilized to monitor the pressure of soil and grout during the injection process. A high-resolution camera records the changes in the injection area during the test. Four different pressure states (Table 1) were designed to examine the effect of injection pressure, and the test is conducted according to these four schemes. The grading curve diagram for the utilized soil in tests is shown in Fig. 3. The laboratory results such as Bleeding, Marsh funnel test and Gelling time for the grout sample are summarized in Table 2.

The test procedure is as follows:

In the first step, the soil with a specific grading is poured into the soil tank, and three percussions were applied to create the required density in the soil (according to ASTM D1557) [32]:

- The grout (mixture of water, cement, and bentonite) is prepared and added to the grout tank;
- The sodium silicate is provided separately and poured inside the corresponding tank;

Table 1 The Utilized schemes in the injection test

Scheme No.	Cement (Kg)	Water (L)	Bentonite (Kg)	Sodium Silicate (Kg)	SiO ₂ /Na ₂ O ratio	W:C	Pressure inside the frame (bar)	Injection Pressure (bar)
1	360	799	40	90	3.1	2.22	0.5	1.5
2	360	799	40	90	3.1	2.22	0.5	2
3	360	799	40	90	3.1	2.22	0.5	2.5
4	360	799	40	90	3.1	2.22	0.5	3



Fig. 2 Injection simulation device

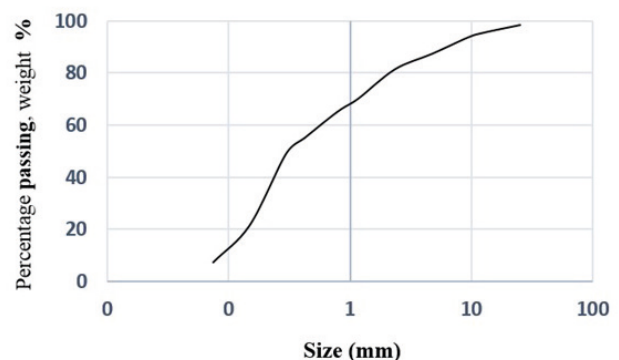


Fig. 3 The grading curve diagram for the utilized soil

Table 2 Bleeding amount in different designs

Design No.	Bleeding (%)	Bleeding Under 5%	Marsh funnel	Marsh funnel status (s)	Gelling time (s)
1	4	Acceptable	36	Acceptable	30

- The air pressure inside the grout and sodium silicate tanks is adjusted to the desired pressures (2, 2.5, and 3 bar);
- The air pressure inside the soil tank is adjusted to the desired pressure;
- The monitoring system is installed;
- The injection process starts.

The thickness of injected area inside the soil tank is measured.

The thickness of injected areas at different injection pressures is indicated in Fig. 4 for all four schemes. The grout spread inside the soil tank and soil layers through the tail spaces among the soil particles. At first, the grout spread was fast toward down, and over time the center of the injected area constantly moved downward. As the injection time passes, the spreading speed of the grout gradually decreases. Therefore, the final shape at the end of the injected area is almost a cylinder.

The grout viscosity was low at the early steps, though it has a high flowability. Thus, the grout spread and penetration are done quickly. At the final step, the grout's viscosity increases rapidly; consequently, the impact of viscous resistance on the grout spread gradually increases. Eventually, the shape of the grout-injected area gradually transforms into a cylinder. As illustrated in Fig. 4, the grout penetrated the tail space among the soil particles and turned into a relatively uniform body. The grouted body has good integrity and relatively high strength. The border of the grouted area was quite rough. By comparing the diffusion process in all four conditions, it can be concluded



Fig. 4 The injected area in the form of a cylinder for various grout pressure (a) 1.5 bar, (b) 2 bar, (c) 2.5 bar, (d) 3 bar

that the impact of injection pressure on the grout spread in the fourth scheme was significantly higher than in the first one. In other words, the grout has penetrated more into the soil in the fourth scheme.

Based on the results provided in Table 3, the penetration rate increases with the increase of injection pressure. For a better understanding of the process of changes, the penetration versus injection pressure is illustrated in Fig. 5.

It can be concluded from the figure that increasing the injection pressure can increase the penetration depth of grout into the soil, so the grout penetration increased from 2.2 cm to 2.9 cm (almost a 30 percent increase) by increasing the pressure from 1.5 bar to 3 bar. This could be considered in situations that need more penetration into the surrounding soil, for example, the TBM in the entry station or to provide sealing around the sealing ring.

3 Numerical modeling

The FLAC3D software is based on finite difference numerical method and developed for engineering calculations and analyses. The capabilities of this software in the three-dimensional mode have been increased compared to the two-dimensional mode and simulate the 3D behavior of structure, soil or rocky ground, or other cases having plastic flow when reaching the yield point. This study used the FLAC3D finite difference software to investigate the impact of changes in the mixture of soil and grout on the ground surface settlement at station 5 of the second line of the Tabriz metro [3].

Table 3 The grout penetration depth in the studied soil

Scheme No.	Pressure inside the frame (bar)	Injection Pressure (bar)	Penetration (cm)
1	0.5	1.5	2.2
2	0.5	2	2.5
3	0.5	2.5	2.6
4	0.5	3	2.9

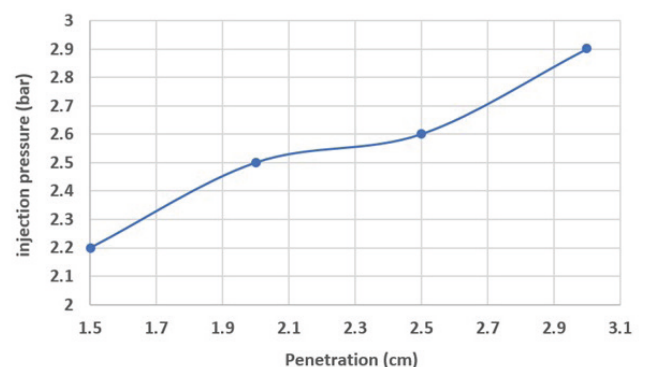


Fig. 5 Penetration depth versus pressure change

For this purpose, the laboratory results were utilized in the software for modeling the injected grout.

Modeling by the FLAC3D software is presented in Fig. 6. As observed, the model geometry is produced in the first step, including the tunnel with a diameter of 9.49 m, along with the grout injection space and the segment. An appropriate behavioral model is selected in the next step. In this case, the selected model is the Mohr–Coulomb model. After that, the characteristics corresponding to the selected behavioral model (density, modulus of elasticity, Poisson's ratio, cohesion, internal friction angle, etc.) are entered into the software. Then, it came to create an initial balance in the model, and the excavation process starts after the balance is established. Moreover, finally the segment injection and installation system are executed.

The created 3D numerical model in the FLAC3D software at the chainage 3+000 km (Line 2 of Tabriz metro) has 80 meters long (along the X axis), 60 meters wide (along the Y axis), and 55 m height (along the Z axis). The tunnel diameter and the excavation length are considered 9.49 m and 40 m, respectively.

The depth of the tunnel overhead is 15.77 m. The 3D geometrical model is illustrated in Fig. 7(a). The applied surface load is 20 KPa (equal to the urban traffic load). The number of zones and grid points created in the model was 53760 and 56334, respectively. The dimensions of meshes get larger as moving away from the tunnel. A design of the boring machine, along with the tunnel and machine specifications, is illustrated in Fig. 7(b). The properties of the retaining system and EPBM are presented in Table 4 [33].

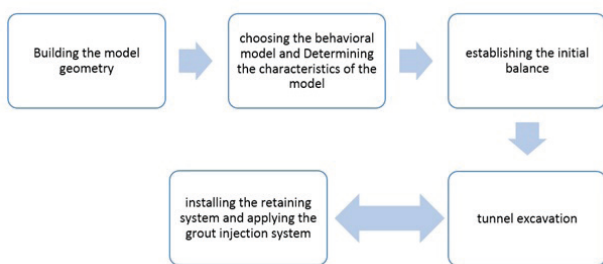


Fig. 6 The flowchart of numerical modeling steps

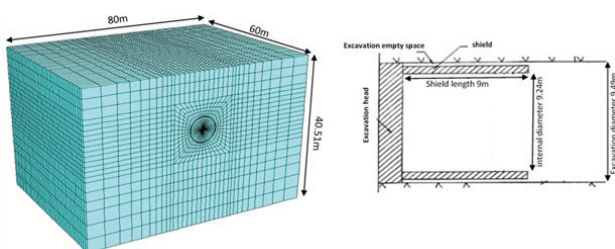


Fig. 7 (a) Dimensions of the model created in FLAC3D software, (b) a design of TBM

The behavioral model of Mohr–Coulomb has been used in modeling this section. The applied characteristics in the FLAC3D software for layers based on the behavioral model of Mohr–Coulomb in the investigating section are presented in Table 5. These characteristics are provided according to the excavated boreholes in the study area.

The main goal in this section is to investigate the effect of grout penetration on the ground surface settlement. Accordingly, the volumetric element with elastic behavior has been used in modeling the injection grout between the precast concrete segment and the surrounding soil. The characteristics of injection grout are adopted based on the experimental results (uniaxial compression test).

Therefore, three schemes with different penetration amounts for the injection grout were modeled.

The built model is balanced after creating and applying the ground characteristics and other parameters and before the start of tunnel excavation. The unbalancing forces and normal stress contours are illustrated in Fig. 8 after the balance. As can be seen from the figure, the stresses are increasing uniformly with the increase of depth. In tunnel excavation modeling, the job started by excavating 1.5 m. Then, we applied the face support pressure and prepared the shield condition at the 1.5 m excavation to install the retention.

Table 4 General characteristics of EPBM in Line 2 of Tabriz metro

Characteristics	Unit	Value
Excavation diameter	meter	9.49
Shield length	meter	9
Shield weight	ton	625
Tale weight	ton	350
Width of the retaining system	meter	1.5
Thickness of retaining system	meter	0.35
Internal diameter	meter	8.48
Thickness of the injection area behind the segment	meter	0.15
External diameter	meter	9.18

Table 5 Characteristics of Soil layers in the study area

Layers	Dominant type	Thickness (m)	Modulus of elasticity (Kg/cm ²)	Density	Ø°	Cohesion (kPa)	Poisson's ratio
1	(SC-SM)	6	400	1650	26	10	0.31
2	(ML, CL)	8	600	1540	24	20	0.35
3	(SM)	6	700	2060	28	15	0.30
4	(ML, CL)	16	800	1940	24	30	0.44
5	Marl	19	800	2150	22	50	0.37

This process continued for 9 meters (as long as the shield length). Then as the shield advances to the length of 10.5 m, the concrete cover and injection behind the concrete cover are applied to the model at the 10.5 m to 12 m of tunnel beginning, and this process was repeated until the end of tunnel excavation. By advancing in the tunnel, the weight of the shield and tail was exerted on the lower quarter of the tunnel. The excavation section, the segment, and the installed shield for the studying part are illustrated in Fig. 9.

The characteristics utilized in the numerical modeling for this section are provided in Table 6. The penetration depth of 25 cm has been chosen considering the difference between the actual dimensions of the tail space behind the segment (15 cm) and the tail space available in the laboratory modeling (4.5 cm) and the scale rules. The penetration depth of 45 cm is also considered as the maximum possible penetration depth. The properties of the mixture of injection grout and soil which is presented in this table have been adopted based on laboratory results. Elastic behavior model is considered for this material.

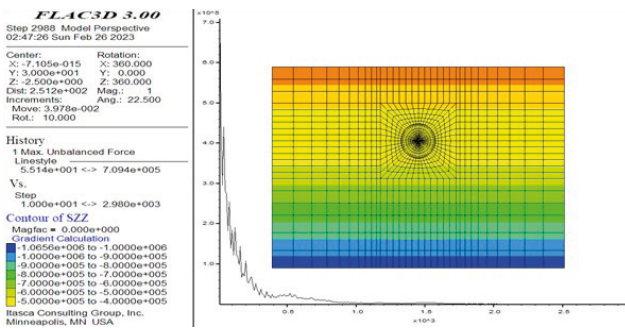


Fig. 8 Diagram of unbalancing forces and vertical stress tensor after the primary balance of model

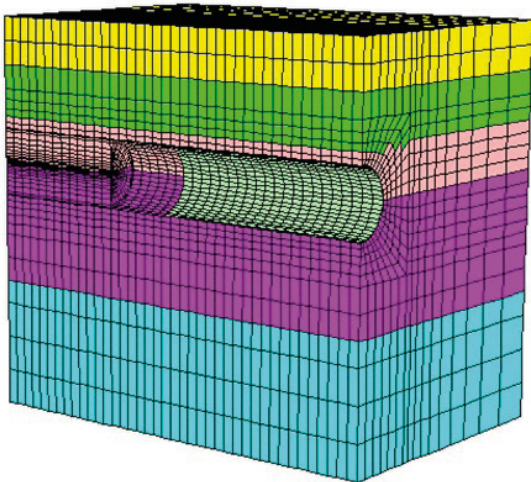


Fig. 9 Modeling after the excavation and installing the retention system

The schematic diagram of the grout thickness is shown in Fig. 10. Different percentages of soil have been used for this purpose. Only the grout properties are entered for the normal case (15 cm). For the case of 25 cm, in addition to the thickness of 15 cm of mere grout, the properties of a 30 % mixture of the grout and soil (the percentage of mixing has been determined based on laboratory studies) have been used for the next 10 cm. In the case of 45 cm, the properties of the mere grout have been selected in the same way for the first 15 cm, the properties of grout mixture with 30% soil for the next 10 cm, and the properties of grout mixture with 20% soil for the next 20 cm.

Based on the settlement measuring provided by Line 2 of Tabriz metro at the chainage 3+000, the settlement amount after the tunnel excavation was 5 mm. Therefore, according to the comparison presented in Table 7, it can be concluded that the numerical modeling has provided an acceptable answer in this section. Thus, further investigations can be done using this numerical modeling. The reduction of surface settlements due to increased grout strength is indicated in Table 7. Based on the modeling results, the amount of ground displacements and, consequently, the surface settlements have decreased at the tail space behind the segment cover of the tunnel by increasing the grout characteristics and strength. The vertical displacement contours for all three models are investigated in Fig. 11.

The changes in ground surface settlement perpendicular to the tunnel axis are shown in Fig. 12 for all three chosen schemes. It can be concluded that the settlement amount can significantly be reduced by increasing the

Table 6 Utilized grout characteristics at each modeling

Scheme No.	Thickness(cm)	Grout mixture	Average of compressive strength (MPa)	Shear (MPa)	Bulk (MPa)	Poisson's ratio	Modulus of elasticity (Kg/cm ²)
1	15	mere grout	0.395	3697.81	8011.93	0.3	9614.325
2	25	30% soil mix	1.4814	6985.20	15134.61	0.3	18161.54
3	45	20% soil mix	0.7877	5081.31	11009.51	0.3	13211.42

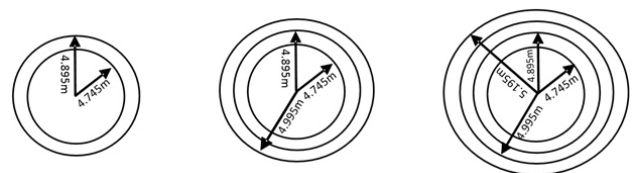


Fig. 10 The schematic diagram of the grout section for all three models

Table 7 Displacements perpendicular to the tunnel axis in all three models

Scheme No.	Maximum displacement perpendicular to the tunnel axis (mm)
1	-5.73
2	-3.68
3	-3.12

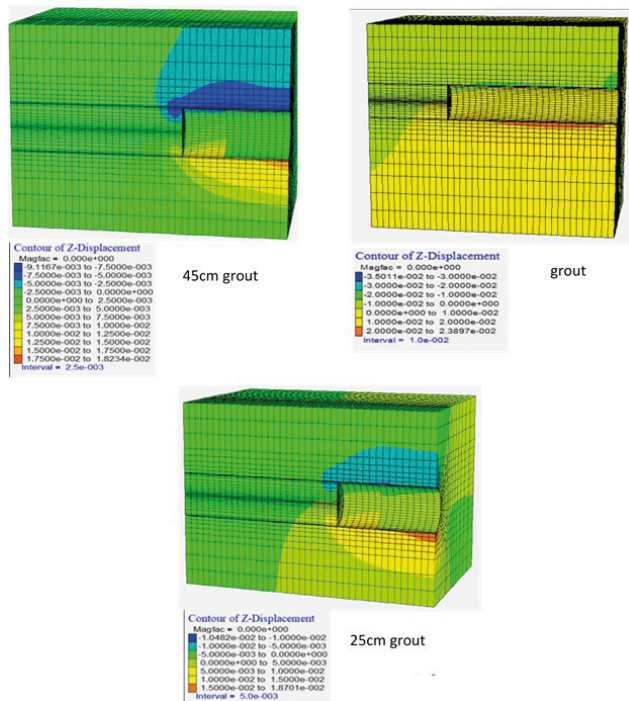


Fig. 11 Displacement contours in three different models

thickness of the grout injection due to the increase in injection pressure. So, the maximum settlement decreased by 80 percent, with an increase of 30 cm for the grout penetration into the soil around the tunnel.

Increasing the injection depth in the coarse-graded soils to reduce the soil's settlement and permeability would be possible.

4 Conclusions

The present study investigates the influence of injection grout penetration into the soil around the tunnel on the ground surface settlement during mechanized excavation with EPBM. First, the amount of grout penetration around

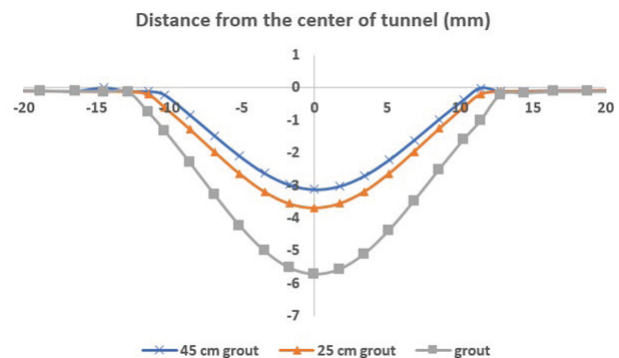


Fig. 12 Displacements perpendicular to the tunnel axis

the tail space was investigated with laboratory studies. Then, its effect on surface settlement has been investigated according to the amount of grout penetration and the percentage of mixing using numerical modeling. So, for this purpose, various experiments were conducted with different mix designs. The obtained results are as follows:

Increasing the injection pressure would increase the amount of grout penetration into the compacted soil. so that by increasing the pressure from 1.5 to 3 bar, the grout penetration increased about 30%.

At first, the spreading speed of the grout spread was high, and over time the center of the injected area constantly moved downward. As the injection time passes, the spreading speed of the grout gradually decreases.

Increasing the depth of injection in coarse-grained soils in order to reduce the amount of settlement and also to reduce the permeability of the soil from the tail space of EPBM is possible.

The presence of pressure in the soil part of the permeability cell increases the grout penetration.

A three-dimensional model was produced for investigating the ground settlement during the excavation in terms of grot injection behind the segment cover of the tunnel at Line 2 of Tabriz metro. The thickness of the injected grout behind the segment cover and its characteristics were examined, and the obtained results were compared with each other and with the field results.

The numerical modeling indicated that increasing the injection depth by increasing the injection pressure would decrease the ground surface settlement by about 80 % and reduce the soil permeability.

References

[1] Wu, T., Gao, Y., Zhou, Y. "Application of a novel grouting material for pre-reinforcement of shield tunnelling adjacent to existing piles in a soft soil area", *Tunnelling and Underground Space Technology*, 128, 104646, 2022. <https://doi.org/10.1016/j.tust.2022.104646>

[2] Guglielmetti, V., Grasso, P., Mahtab, A., Xu, S. (Eds.) "Mechanized tunnelling in urban areas: design methodology and construction control", CRC Press, 2008. ISBN: 9780203938515 <https://doi.org/10.1201/9780203938515>

- [3] Sharghi, M., Chakeri, H., Ozcelik, Y. "Investigation into the effects of two component grout properties on surface settlements", *Tunnelling and Underground Space Technology*, 63, pp. 205–216, 2017.
<https://doi.org/10.1016/j.tust.2017.01.004>
- [4] Youn, B. Y., Breitenbücher, R. "Influencing parameters of the grout mix on the properties of annular gap grouts in mechanized tunneling", *Tunnelling and Underground Space Technology*, 43, pp. 290–299, 2014.
<https://doi.org/10.1016/j.tust.2014.05.021>
- [5] Moseley, M.P., Kirsch, K. (Eds.) "Ground improvement", CRC Press, 2004. ISBN: 9780429095917
<https://doi.org/10.1201/9780203489611>
- [6] Vonk, M. "Grouting the tail void: Analysis of the tail void grouting process at the North/South line", Mac Thesis, Delft University of Technology, 2020. [online] Available at: <http://resolver.tudelft.nl/uuid:9def2b0f-b3db-4cb0-9dc1-d0a77692e53d>
- [7] Karbalayi, M. A., Katibeh, H. "Injectability studies", In: *Cement grout injection into rock*, Tarava, 2009, pp. 107–133. ISBN: 6005620010 (In Persian)
- [8] André, L., Bacquié, C., Comin, G., Ploton, R., Achard, D., Frouin, L., Cyr, M. "Improvement of two-component grouts by the use of ground granulated blast furnace slag", *Tunnelling and Underground Space Technology*, 122, 104369, 2022.
<https://doi.org/10.1016/j.tust.2022.104369>
- [9] Song, W., Zhu, Z., Pu, S., Wan, Y., Huo, W., Peng, Y. "Preparation and engineering properties of alkali-activated filling grouts for shield tunnel", *Construction and Building Materials*, 314, 125620, 2022.
<https://doi.org/10.1016/j.conbuildmat.2021.125620>
- [10] Mansour, M. A. M. "Three-dimensional numerical modelling of hydroshield tunnelling", PhD Thesis, University of Innsbruck, 1996.
- [11] Abu-Krishna, A. A. M. "Numerical modelling of TBM tunneling in consolidated clay", PhD Thesis, University of Innsbruck, 1998.
- [12] Greenwood, J. D. "Three-dimensional analysis of surface settlement in soft ground tunneling", BSc Thesis, Massachusetts Institute of Technology, 2003. [online] Available at: <http://hdl.handle.net/1721.1/29558>
- [13] Kasper, T., Meschke, G. "On the influence of face pressure, grouting pressure and TBM design in soft ground tunneling", *Tunnelling and Underground Space Technology*, 21(2), pp. 160–171, 2006.
<https://doi.org/10.1016/j.tust.2005.06.006>
- [14] Nagel, F., Meschke, G. "Grout and bentonite flow around a TBM: Computational modeling and simulation-based assessment of influence on surface settlements", *Tunnelling and Underground Space Technology*, 26(3), pp. 445–452, 2011.
<https://doi.org/10.1016/j.tust.2010.12.001>
- [15] Lambrughi, A., Rodríguez, L. M., Castellanza, R. "Development and validation of a 3D numerical model for TBM–EPB mechanised excavations", *Computers and Geotechnics*, 40, pp. 97–113, 2012.
<https://doi.org/10.1016/j.compgeo.2011.10.004>
- [16] Li, Z., Grasmick, J., Mooney, M. "Influence of slurry TBM parameters on ground deformation", presented at the ITA WTC 2015 Congress and 41st General Assembly, Dubrovnik, Croatia, May, 22–28, 2015.
- [17] Oh, J.-Y., Ziegler, M. "Investigation on influence of tail void grouting on the surface settlements during shield tunneling using a stress-pore pressure coupled analysis", *KSCE Journal of Civil Engineering*, 18, pp. 803–811, 2014.
<https://doi.org/10.1007/s12205-014-1383-8>
- [18] Shah, R., Lavasan, A. A., Peila, D., Todaro, C., Luciani, A., Schanz, T. "Numerical study on backfilling the tail void using a two-component grout", *Journal of Materials in Civil Engineering*, 30(3), 04018003, 2018.
[https://doi.org/10.1061/\(ASCE\)MT.1943-5533.0002175](https://doi.org/10.1061/(ASCE)MT.1943-5533.0002175)
- [19] Ochmański, M., Modoni, G., Bzówka, J. "Automated numerical modelling for the control of EPB technology", *Tunnelling and Underground Space Technology*, 75, pp. 117–128, 2018.
<https://doi.org/10.1016/j.tust.2018.02.006>
- [20] Loganathan, N., Poulos, H. G. "Analytical prediction for tunneling-induced ground movements in clays", *Journal of Geotechnical and Geoenvironmental Engineering*, 124(9), pp. 846–856, 1998.
[https://doi.org/10.1061/\(ASCE\)1090-0241\(1998\)124:9\(846\)](https://doi.org/10.1061/(ASCE)1090-0241(1998)124:9(846))
- [21] Komiya, K., Soga, K., Akagi, H., Jafari, M. R., Bolton, M. D. "Soil consolidation associated with grouting during shield tunnelling in soft clayey ground", *Géotechnique*, 51(10), pp. 835–846, 2001.
<https://doi.org/10.1680/geot.2001.51.10.835>
- [22] Liu, X.-X., Shen, S.-L., Xu, Y.-S., Zhou, A. "Non-linear spring model for backfill grout-consolidation behind shield tunnel lining", *Computers and Geotechnics*, 136, 104235, 2021.
<https://doi.org/10.1016/j.compgeo.2021.104235>
- [23] Mohammadzamani, D., Lavasan, A. A., Wichtmann, T. "Tail void grouting material: A parametric study on the role of hydro-mechanical characteristics in mechanized tunneling", *Tunnelling and Underground Space Technology*, 135, 105053, 2023.
<https://doi.org/10.1016/j.tust.2023.105053>
- [24] Xue, X., Zhang, K., Ma, B., Xiao, F., Jiang, T. "Numerical simulating of pregrouting in multi-jointed rock mass in deep coalmine roadway excavated via TBM", *Computers and Geotechnics*, 154, 105166, 2023.
<https://doi.org/10.1016/j.compgeo.2022.105166>
- [25] Liu, Y., Hou, S., Li, C., Zhou, H., Jin, F., Qin, P., Yang, Q. "Study on support time in double-shield TBM tunnel based on self-compacting concrete backfilling material", *Tunnelling and Underground Space Technology*, 96, 103212, 2020.
<https://doi.org/10.1016/j.tust.2019.103212>
- [26] Chakeri, H., Balani, A., Sharghi, M., Özcelik, Y. "An Investigation into the Effects of an Annular Gap on Surface Settlement", *Soil Mechanics and Foundation Engineering*, 57, pp. 506–512, 2021.
<https://doi.org/10.1007/s11204-021-09699-y>
- [27] Rahmati, S., Chakeri, H., Sharghi, M., Dias, D. "Experimental study of the mechanical properties of two-component backfilling grout", *Proceedings of the Institution of Civil Engineers-Ground Improvement*, 175(4), pp. 277–289, 2022.
<https://doi.org/10.1680/jgrim.20.00037>
- [28] Oreste, P., Spagnoli, G. "The characteristics of the two-component grout on the stress-state in segmental lining", *Geotechnical and Geological Engineering*, 2023.
<https://doi.org/10.1007/s10706-023-02615-1>

- [29] Todaro, C., Saltarin, S., Cardu, M. "Bentonite in two-component grout applications", *Case Studies in Construction Materials*, 16, e00901, 2022.
<https://doi.org/10.1016/j.cscm.2022.e00901>
- [30] Todaro, C., Martinelli, D., Boscaro, A., Carigi, A., Saltarin, S., Peila, D. "Characteristics and testing of two-component grout in tunnelling applications", *Geomechanics and Tunnelling*, 15(1), pp. 121–131, 2022.
<https://doi.org/10.1002/geot.202100019>
- [31] Todaro, C., Pace, F. "Elastic properties of two-component grouts at short curing times: The role of bentonite", *Tunnelling and Underground Space Technology*, 130, 104756, 2022.
<https://doi.org/10.1016/j.tust.2022.104756>
- [32] ASTM "D1557-12(2021) Standard Test Methods for Laboratory Compaction Characteristics of Soil Using Modified Effort (56,000 ft-lbf/ft³ (2,700 kN-m/m³))", ASTM International, West Conshohocken, PA, USA, 2021.
<https://doi.org/10.1520/D1557-12R21>
- [33] Narimani, S., Chakeri, H., Davarpanah, S. M. "Simple and non-linear regression techniques used in sandy-clayey soils to predict the pressuremeter modulus and limit pressure: A case study of Tabriz subway", *Periodica Polytechnica Civil Engineering*, 62(3), pp. 825–839, 2018.
<https://doi.org/10.3311/PPci.12063>